Recursive Least Squares Channel Estimator with Smoothing and Removing for Iterative-MAP Receiver of MIMO-OFDM Mobile Communications

Tsuyoshi KASHIMA, Kazuhiko FUKAWA, and Hiroshi SUZUKI
Tokyo Institute of Technology
2-12-1, O-okayama, Meguro-ku, Tokyo, 152-8550 Japan
E-mail: {tsuyoshi.kashima, fukawa, suzuki}@radio.ss.titech.ac.jp

***Abstract*— This paper proposes novel channel estimation methods for an iterative maximum *a posteriori* (MAP) receiver. The targeted systems are low-density parity-check (LDPC)-coded multiple-input-multiple-output (MIMO) and orthogonal frequency-division multiplexing (OFDM) mobile communications. By reconsidering the joint processing of the iterative MAP receiver from the viewpoint of the message-passing algorithm in the factor graph, this paper theoretically derives the recursive least squares (RLS) algorithm with *smoothing* and *removing* (SR-RLS). The computational complexity of SR-RLS is about two to three times larger than that of the original RLS algorithm. Computer simulations under fast multipath fading conditions show that the MAP receiver using the proposed SR-RLS channel estimator outperforms the one using the conventional RLS channel estimator.**

I. Introduction

As a transmission scheme to achieve a high bit-rate and high spectral-efficient mobile communication, orthogonal frequency-division multiplexing (OFDM) has attracted much attention because it is a multi-carrier transmission scheme with a guard interval (GI) and can maintain excellent transmission performance even in multipath fading channels. In addition, the multiple-input-multiple-output (MIMO) technique, which spatially multiplexes data streams by multiple antennas, can further increase the spectral efficiency. As a channel code for the MIMO-OFDM system, the low density parity-check (LDPC) code is promising because it can exploit the time, frequency, and space diversity owing to its built-in interleaver, and has great error-correction ability [1], [2].

The optimal signal detection for the LDPC-coded MIMO-OFDM system is based on maximum *a posteriori* (MAP) criteria. However, the MAP receiver requires a prohibitively large amount of computational complexity without any approximation. Thus, this paper considers an iterative MAP receiver that can reduce the complexity by an iterative approximation method for the LDPC-coded MIMO-OFDM system.

As one of the iterative methods, the expectation-maximization (EM) algorithm [3], [4] has been studied, which performs the signal detection and the channel estimation iteratively so as to asymptotically achieve the MAP detection with practical complexity [5]-[7]. On the basis of the EM algorithm, the iterative MAP receiver with the minimum-mean-square-error (MMSE) channel estimator has been proposed for the LDPC-coded MIMO OFDM system in [8], [9]. The receivers with the recursive least squares (RLS) or the least mean square (LMS) channel estimators have been also proposed to improve the fading tracking ability [15].

As another theoretical background for the iterative joint processing of the signal detection and the channel estimation, the message-passing algorithm in the factor graph is also considered in this paper. Various algorithms such as the Viterbi algorithm, the LDPC decoding, and the Kalman filter including the RLS algorithm can be derived from the message-passing algorithm [10], [11]. By reconsidering the joint processing from the message-passing viewpoint, this paper and [16] propose new channel estimation methods such as *smoothing* and *removing*. In addition to the discussion of [16], this paper also explains the theoretical derivation of these new proposed channel estimation algorithms in detail.

The rest of this paper is organized as follows. Section II presents the system model of the MIMO-OFDM system, and Section III describes the iterative MAP receiver structure. In Section IV, the factor graph representations of the system and the derivation of the novel channel estimation algorithms are detailed. Section V shows computer simulation results of the proposed iterative MAP receivers. Finally, some concluding remarks are given in Section VI.

II. System Model

Let us consider an LDPC-coded MIMO-OFDM system with N_T transmitter antennas, N_R receiver antennas, N subcarriers, and N_S OFDM symbols in one packet. In the MIMO-OFDM transmitter, the LDPC-encoded bit sequence of a packet is modulated into a serial symbol sequence, and the serial-parallel transform converts it into $N_T N$ parallel symbol sequences. Let $b_k(i,n)$ denote the transmitted symbol from the k-th $(1 \le k \le N_T)$ transmitter antenna at the n-th $(0 \le n < N)$ sub-carrier in the i-th $(0 \le i < N_S)$ OFDM symbol. Each set of N parallel symbols is passed into the inverse fast Fourier transform (IFFT) corresponding to each transmitter antenna, and GI is added to its output every OFDM symbol. With the OFDM sampling interval Δ_t as a time unit, the GI length is given by $\Delta_G \Delta_t$. Thus, the transmitted symbol $s_k(m)$ from the k-th transmitter antenna at discrete time $m\Delta_t$

can be expressed as

$$s_k(m) = \sum_{n=0}^{N-1} b_k(i,n) \exp\left\{ j \frac{2\pi n[m-(i+1)\Delta_G]}{N} \right\}, \quad (1)$$

where $i(N+\Delta_G) \le m < (i+1)(N+\Delta_G)$.

Let us assume that every channel between transmitter and receiver antennas is subject to uncorrelated multi-path Rayleigh fading and is also spatially uncorrelated to each other. The channel impulse response, $h_{kl}(t;\tau)$, between the k-th transmitter antenna and the l-th receiver antenna at time t as a function of delay time τ can be modeled as

$$h_{lk}(t;\tau) = \sum_{d=0}^{D} \alpha_{lk,d}(t)\delta(\tau - d\Delta_t) \quad (2)$$

where $D\Delta_t$ is the maximum delay time, $\alpha_{kl,d}(t)$ represents the Rayleigh-fading complex envelope on the d-th propagation path between the k-th transmitter antenna and the l-th receiver antenna at time t, and $\delta(\cdot)$ is the Dirac delta function. In the MIMO-OFDM receiver, the signal received by the l-th receiver antenna at discrete time $m\Delta_t$, which is $y_l(m)$, is given by

$$y_l(m) = \sum_{k=1}^{N_T} \sum_{d=0}^{D} \alpha_{lk,d}(m\Delta_t) s_k(m-d) + n_l(m) \quad (3)$$

where $n_l(m)$ is the noise of the l-th receiver antenna at discrete time $m\Delta_t$, $0 \le m < N_m$, and $N_m = N_S(N+\Delta_G)$. The GI is removed from the received signal of each receiver antenna every OFDM symbol, and the resultant signal is fed into the corresponding fast Fourier transform (FFT). $Y_l(i,n)$ denotes the FFT output of the l-th receiver antenna at the n-th subcarrier in the i-th OFDM symbol, and can be expressed as

$$Y_l(i,n) = N^{-1} \sum_{m=i(N+\Delta_G)+\Delta_G}^{(i+1)(N+\Delta_G)-1} y_l(m) \exp\left\{ -j \frac{2\pi n[m-(i+1)\Delta_G]}{N} \right\}. \quad (4)$$

On the assumption that the maximum delay time is not longer than GI, that is $D \le \Delta_G$, and that $\alpha_{lk,d}(m\Delta_t)$ is constant during one OFDM symbol, substituting (1) and (3) into (4) approximately yields

$$Y_l(i,n) = \sum_{k=1}^{N_T} H_{lk}(i,n) b_k(i,n) + N_l(i,n) \quad (5)$$

$$H_{lk}(i,n) = \sum_{d=0}^{D} \alpha_{lk,d}[m_{\mathrm{a}}(i)\Delta_t] \exp\left(-j \frac{2\pi n d}{N} \right) \quad (6)$$

$$N_l(i,n) = N^{-1} \sum_{m=i(N+\Delta_G)+\Delta_G}^{(i+1)(N+\Delta_G)-1} n_l(m) \exp\left\{ -j \frac{2\pi n[m-(i+1)\Delta_G]}{N} \right\} \quad (7)$$

where $\alpha_{lk,d}[m_{\mathrm{a}}(i)\Delta_t]$ is the average value of $\alpha_{lk,d}(m\Delta_t)$ in the i-th OFDM symbol, and $m_{\mathrm{a}}(i) = i(N+\Delta_G)+\Delta_G+N/2$ is assumed in this paper. Note that the channel variation in one OFDM symbol, which this model neglects, causes interference between subcarriers and that its effect will be considered in simulation results.

The demodulation uses the frequency-domain signal model of (5) in the vector form as

$$\begin{aligned} Y_l(i,n) &= \mathbf{H}_l^{\mathrm{H}}(i,n)\mathbf{X}(i,n) + N_l(i,n) \quad (8)\\ \mathbf{H}_l^{\mathrm{H}}(i,n) &= [H_{l1}(i,n), \cdots, H_{lN_T}(i,n)], \\ \mathbf{X}^{\mathrm{H}}(i,n) &= \left[b_1^*(i,n), \cdots, b_{N_T}^*(i,n)\right] \end{aligned}$$

where $\mathbf{H}_l(i,n)$ and $\mathbf{X}(i,n)$ are N_T-by-1 vectors, and $^{\mathrm{H}}$ and * denote Hermitian transposition and complex conjugate, respectively. Furthermore, an N-by-1 vector $\mathbf{Y}_l(i)$ having $Y_l(i,n)$ as its elements is given by

$$\begin{aligned} \mathbf{Y}_l(i) &= \mathbf{X}^{\mathrm{H}}(i)\mathbf{H}_l(i) + \mathbf{N}(i), \quad (9)\\ \mathbf{Y}_l^{\mathrm{H}}(i) &= [Y_l^*(i,1), \cdots, Y_l^*(i,N)], \\ \mathbf{N}^{\mathrm{H}}(i) &= [N_l^*(i,1), \cdots, N_l^*(i,N)] \\ \mathbf{X}^{\mathrm{H}}(i) &= [\mathbf{X}_1(i), \cdots, \mathbf{X}_{N_T}(i)], \\ \mathbf{X}_k(i) &= \mathrm{diag}\,[b_k(i,1), \cdots, b_k(i,N)], \\ \mathbf{H}_l^{\mathrm{H}}(i) &= [H_{l1}^*(i,1), \cdots, H_{l1}^*(i,N), \cdots, \\ & \quad H_{lN_T}^*(i,1), \cdots, H_{lN_T}^*(i,N)], \end{aligned}$$

where $\mathbf{Y}_l(i)$ and $\mathbf{N}(i)$ are N-by-1 vectors, $\mathbf{H}_l(i)$ is an NN_T-by-1 vector, $\mathbf{X}(i)$ is an NN_T-by-N matrix, and $\mathrm{diag}[\,]$ denotes a diagonal matrix consisting of its arguments.

On the other hand, the channel estimation uses the time-domain signal model of (3) for more accurate estimation. It is expressed in the vector form as

$$\begin{aligned} y_l(m) &= \mathbf{h}_l^{\mathrm{H}}(m)\mathbf{x}(m) + n_l(m) \quad (10)\\ \mathbf{h}_l^{\mathrm{H}}(m) &= [\alpha_{l1,0}(m\Delta_t), \cdots \alpha_{l1,D}(m\Delta_t), \cdots \\ & \quad \alpha_{lN_T,0}(m\Delta_t), \cdots \alpha_{lN_T,D}(m\Delta_t)] \\ \mathbf{x}^{\mathrm{H}}(m) &= [s_1^*(m), \cdots s_1^*(m-D), \cdots \\ & \quad s_{N_T}^*(m), \cdots s_{N_T}^*(m-D)] \end{aligned}$$

where $\mathbf{h}_l(m)$ and $\mathbf{x}(m)$ are $(D+1)N_T$-by-1 vectors.

For simplicity, the receiver antenna index l will be omitted below.

III. Iterative MAP receiver

A. Receiver Framework

The receiver performs a joint processing of channel estimation, demodulation and channel decoding. The whole receiver process consists of the initialization and iteration steps.

The initialization step in Fig. 1 is performed only once. Starting from the preamble symbols, the channel and the symbol are estimated and detected alternately symbol-by-symbol. It is performed recursively from the front to the end of a packet. The symbol detection is based on the maximum likelihood (ML) criteria, and produces the log likelihood ratio (LLR) $\lambda_1(p)$ of every p-th coded bit. Given $\lambda_1(p)$, the LDPC decoder maximizes *a posteriori* LLR $\lambda_3(p)$, and returns *a priori* LLR $\lambda_2(p) = \lambda_3(p) - \lambda_1(p)$.

The iteration step in Fig. 1, which is referred to as the inner loop, is performed after the initialization step. The channel for the whole packet is estimated by using the hard decision of $\lambda_3(p)$. Then, using the estimated channel and $\lambda_2(p)$ from the LDPC decoder, the MAP demodulator maximizes $\lambda_3(p)$, and produces $\lambda_1(p) = \lambda_3(p) - \lambda_2(p)$. After the inner loop iteration, $\lambda_1(p)$ is passed to the LDPC decoder, and the LDPC decoder maximizes $\lambda_3(p)$ again. The iteration between the inner loop and the LDPC decoder is referred to as the outer loop. The outer loop iteration repeats unless the LDPC-parity check is passed or the iteration number exceeds a predetermined number, and the inner loop iteration repeats unless the iteration number exceeds another predetermined number.

B. MAP Symbol Detection of the inner loop

The inner loop iteration follows the EM algorithm in the same way as [15], [16], and the detected symbol at the $(r+1)$-th inner loop iteration, $\mathbf{X}^{(r+1)}$, can be expressed as

$$\text{E step}: \quad q[\mathbf{X}(i,n)|\mathbf{X}^{(r)}] = \tag{11}$$
$$-\frac{|Y(i,n) - \hat{\mathbf{H}}^{\mathrm{H}}(i,n)\mathbf{X}(i,n)|^2}{\sigma^2} - \frac{\mathbf{X}^{\mathrm{H}}(i,n)\boldsymbol{\Sigma}_{\mathbf{H}}(i,n)\mathbf{X}(i,n)}{\sigma^2}$$
$$\text{M step}: \quad \mathbf{X}^{(r+1)}(i,n) =$$
$$\arg \max_{\mathbf{X}(i,n)} \left\{ q[\mathbf{X}(i,n)|\mathbf{X}^{(r)}] + \log P\left[\mathbf{X}(i,n)\right] \right\} \tag{12}$$

where $\hat{\mathbf{H}}(i,n)$ and $\boldsymbol{\Sigma}_{\mathbf{H}}(i,n)$ are the average and the covariance matrix of $\mathbf{H}(i,n)$, respectively, which are estimated by using $\mathbf{Y}(i)$ and $\mathbf{X}^{(r)}$. σ^2 represents the average power of $N(i,n)$. In case of the receiver without the inner loop, the MAP demodulation is performed after the channel estimation only once in each outer loop iteration.

C. Channel Estimation

As mentioned in Section II, the channel estimation is performed in the time domain. $\hat{\mathbf{H}}(i,n)$ and $\boldsymbol{\Sigma}_{\mathbf{H}}(i,n)$ can be obtained from the mean $\hat{\mathbf{h}}(m)$ and the covariance matrix $\mathbf{P}(m)$ of the estimation of $\mathbf{h}(m)$. Note that $\mathbf{P}(m)$ is normalized by the average noise power σ^2 for notation simplicity. In order to adaptively track the fast fading channel, the initialization step uses the RLS algorithm in the same way as [15], and the iteration step employs the new proposed channel estimator derived in Section IV.

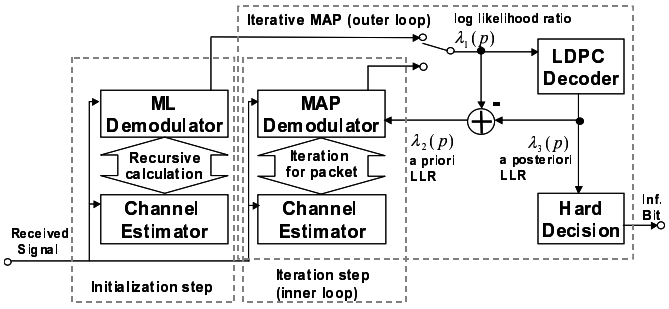

Fig. 1. Structure of the iterative MAP receiver

IV. Derivation of *Smoothing* and *Removing* for the RLS algorithm

In order to investigate the optimal channel estimation algorithm for the iterative MAP receiver, this section discusses it from the factor graph viewpoint.

A. Factor Graph Presentation of the inner loop

The factor graph is a bipartite graph consisting of *local functions* and their arguments called *variables*. In Figs. 2-3, black squares and white circles symbolize the *local functions* and the *variables* respectively in the same way as [10]. A global function of variables can be represented by a factor graph, and can be calculated via the message-passing algorithm on the factor graph. The basic rule of the local message passing is as follows [10], [11]: Each message conveys a conditional probability density function of each *variable*. The out-going message on an edge from a node is generated from the incoming messages on all the other edges to the node. Messages in both directions of all edges need to be calculated every iteration.

Fig. 2 shows the factor graph of the system model where the *variables* correspond to the channel and the symbol information, and the *local functions* correspond to the relations between them. The transmitted symbols and the channel information at the i-th OFDM symbol are rewritten as $\mathbf{X}_i = \mathbf{X}(i)$ and $\mathbf{H}_i = \mathbf{H}(i)$, respectively. The *local function* $\mathrm{f}(\mathbf{H}_i, \mathbf{H}_{i+1})$ represents the relation between the channels at neighboring OFDM symbols, which is equivalent to the random walk model in the case of RLS. Furthermore, the *local function*, $\mathrm{g}_i(\mathbf{H}_i, \mathbf{X}_i)$, represents the relation of (9) at the i-th OFDM symbol.

Fig. 3 shows all the local messaging passings around the node $\mathbf{H}_i$. The arrows from the transmitted symbols and the channels are messages, which are probability distribution functions, such as the likelihood of symbols, and the distribution of channels, respectively. Fig. 3 (a) and (b) correspond to the original, and the opposite-directional RLS channel estimations, respectively. From these two types of message passings, the channel estimation using all detected signals is derived, and this modification is referred to as *smoothing*.

The important finding from the message passing algorithm is in Fig. 3(c), which indicates that the channel for the i-th OFDM symbol detection should be estimated only from the channel of the neighboring symbols without the direct contribution from the i-th OFDM symbol. Then, this is referred to as *removing* in this paper. RLS with *smoothing*,

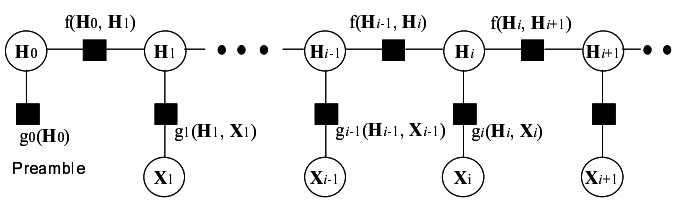

Fig. 2. Factor graph representation of channel and transmitted symbols (RLS)

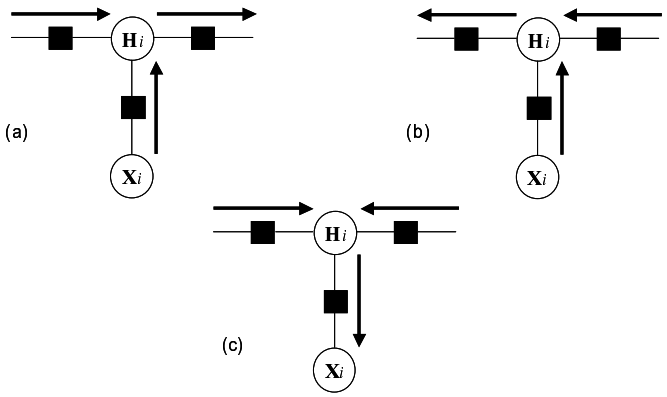

Fig. 3. Local message passings. (a) RLS, (b) smoothing, (c) removing

and RLS with *smoothing* and *removing* are referred to as S-RLS and SR-RLS respectively. By taking the meanings of *smoothing* and *removing*, S-RLS and SR-RLS will be derived in the following subsections. Since the passing of the exact soft messages for both symbols and channels requires high computational complexity, the messages of the symbols are approximated as the symbols having the maximum probability, and the distribution of the channel is approximated as the Gaussian distribution using the mean and the covariance.

B. Derivation of RLS algorithm

As a reference, this subsection derives the original RLS algorithm shown in Fig. 3. Considering the solution of the normal equation that minimizes the mean square errors, $\hat{\mathbf{h}}(m)$ and $\mathbf{P}(m)$ of the RLS estimation are given by

$$\hat{\mathbf{h}}(m) = \mathbf{R}^{-1}(m)\mathbf{V}(m), \quad \mathbf{P}(m) = \mathbf{R}^{-1}(m), \tag{13}$$

$$\mathbf{R}(m) = \sum_{m'=0}^{m} \lambda^{|m-m'|}\mathbf{x}(m')\mathbf{x}^{\mathrm{H}}(m'), \tag{14}$$

$$\mathbf{V}(m) = \sum_{m'=0}^{m} \lambda^{|m-m'|}\mathbf{x}(m')y^{*}(m'). \tag{15}$$

where λ $(0 < \lambda \leq 1)$ is the forgetting factor. By applying the matrix inverse lemma to (13), the recursive formula of $\mathbf{P}(m)$ can be written as

$$\begin{aligned}\mathbf{P}(m) &= \left[\lambda\mathbf{R}(m-1) + \mathbf{x}(m)\mathbf{x}^{\mathrm{H}}(m)\right]^{-1} \\ &= \lambda^{-1}\left[\mathbf{P}(m-1) - \mathbf{K}(m)\mathbf{x}^{\mathrm{H}}(m)\mathbf{P}(m-1)\right], \end{aligned}\tag{16}$$

$$\mathbf{K}(m) = \mathbf{P}(m-1)\mathbf{x}(m)\left[\mathbf{x}^{\mathrm{H}}(m)\mathbf{P}(m-1)\mathbf{x}(m) + \lambda\right]^{-1}. \tag{17}$$

Then, substituting (16) into (13) yields

$$\begin{aligned}\hat{\mathbf{h}}(m) &= \mathbf{P}(m)\left[\lambda\mathbf{V}(m-1) + \mathbf{x}(m)y^{*}(m)\right] \\ &= \hat{\mathbf{h}}(m-1) + \mathbf{K}(m)\left[y^{*}(m) - \mathbf{x}^{\mathrm{H}}(m)\hat{\mathbf{h}}(m-1)\right]. \end{aligned}\tag{18}$$

(16)-(18) are the RLS algorithm procedures, which are recursively performed from $m = 0$ to $N_m - 1$.

C. Derivation of S-RLS

The S-RLS algorithm can be derived in the similar way to the RLS algorithm. First, $\hat{\mathbf{h}}_{\mathrm{s}}(m)$ and $\mathbf{P}_{\mathrm{s}}(m)$ of the S-RLS estimation are defined as

$$\hat{\mathbf{h}}_{\mathrm{s}}(m) = \mathbf{R}_{\mathrm{s}}^{-1}(m)\mathbf{V}_{\mathrm{s}}(m), \quad \mathbf{P}_{\mathrm{s}}(m) = \mathbf{R}_{\mathrm{s}}^{-1}(m), \tag{19}$$

$$\mathbf{R}_{\mathrm{s}}(m) = \sum_{m'=0}^{N_m-1} \lambda^{|m-m'|}\mathbf{x}(m')\mathbf{x}^{\mathrm{H}}(m'), \tag{20}$$

$$\mathbf{V}_{\mathrm{s}}(m) = \sum_{m'=0}^{N_m-1} \lambda^{|m-m'|}\mathbf{x}(m')y^{*}(m'). \tag{21}$$

Applying the matrix inverse lemma to (19) results in

$$\begin{aligned}\mathbf{P}_{\mathrm{s}}(m+1) &= \left[\lambda\mathbf{R}(m) + \mathbf{R}'(m)\right]^{-1} \\ &= \lambda^{-1}\mathbf{P}(m) - \lambda^{-2}\mathbf{P}(m)\left[\lambda^{-1}\mathbf{I} + \mathbf{R}(m)\mathbf{R}'^{-1}(m)\right]^{-1} \end{aligned}\tag{22}$$

where $\mathbf{R}'(m) = \mathbf{R}_{\mathrm{s}}(m+1) - \lambda\mathbf{R}(m)$, and $\mathbf{I}$ is an identity matrix. Similarly

$$\begin{aligned}\mathbf{P}_{\mathrm{s}}(m) &= \left[\mathbf{R}(m) + \lambda\mathbf{R}'(m)\right]^{-1} \\ &= \mathbf{P}(m) - \mathbf{P}(m)\left[\mathbf{I} + \lambda^{-1}\mathbf{R}(m)\mathbf{R}'^{-1}(m)\right]^{-1}. \end{aligned}\tag{23}$$

On the other hand, $\hat{\mathbf{h}}_{\mathrm{s}}(m)$ can be obtained from (19)-(21) as

$$\begin{aligned}\hat{\mathbf{h}}_{\mathrm{s}}(m) &= \left[\lambda\mathbf{R}_{\mathrm{s}}(m+1) + (1-\lambda^2)\mathbf{R}(m)\right]^{-1} \\ &\quad \times \left[\lambda\mathbf{V}_{\mathrm{s}}(m+1) + (1-\lambda^2)\mathbf{V}(m)\right] \\ &= \lambda\left[\lambda\mathbf{I} + (1-\lambda^2)\mathbf{P}_{\mathrm{s}}(m+1)\mathbf{P}^{-1}(m)\right]^{-1}\hat{\mathbf{h}}_{\mathrm{s}}(m+1) \\ &\quad + (1-\lambda^2)\left[\lambda\mathbf{P}(m)\mathbf{P}_{\mathrm{s}}^{-1}(m+1) + (1-\lambda^2)\mathbf{I}\right]^{-1}\hat{\mathbf{h}}(m). \end{aligned}\tag{24}$$

From the definition of $\mathbf{R}'(m)$, the following equation holds:

$$\mathbf{P}(m)\mathbf{P}_{\mathrm{s}}^{-1}(m+1) = \mathbf{R}^{-1}(m)\mathbf{R}'(m) + \lambda\mathbf{I}. \tag{25}$$

Hence, using (25), the calculations of (22)-(24) require $\mathbf{R}'(m)\mathbf{R}^{-1}(m)$ or $\mathbf{R}^{-1}(m)\mathbf{R}'(m)$. In order to reduce the computational complexity, we use the approximation that $\mathbf{R}'(m)\mathbf{R}^{-1}(m) = \mathbf{R}^{-1}(m)\mathbf{R}'(m) = \mathbf{I}$. This is reasonable because both $\mathbf{R}'(m)$ and $\mathbf{R}(m)$ have information on the m-th symbol with the maximum weight and on other symbols with exponentially decreasing weight. Then, (22) and (23) can be respectively rewritten as

$$\mathbf{P}_{\mathrm{s}}(m+1) = \lambda^{-1}\mathbf{P}(m) - \lambda^{-2}\mathbf{P}(m)(\lambda^{-1}+1)^{-1}, \tag{26}$$

$$\mathbf{P}_{\mathrm{s}}(m) = \mathbf{P}(m) - \mathbf{P}(m)(1+\lambda^{-1})^{-1}. \tag{27}$$

From (26) and (27),

$$\mathbf{P}_{\mathrm{s}}(m) = \mathbf{P}(m) + \lambda^2\left[\mathbf{P}_{\mathrm{s}}(m+1) - \lambda^{-1}\mathbf{P}(m)\right]. \tag{28}$$

Furthermore, from (24) and (25), $\hat{\mathbf{h}}_{\mathrm{s}}(m)$ can be rewritten as

$$\hat{\mathbf{h}}_{\mathrm{s}}(m) = \hat{\mathbf{h}}(m) + \lambda\left[\hat{\mathbf{h}}_{\mathrm{s}}(m+1) - \hat{\mathbf{h}}(m)\right]. \tag{29}$$

The S-RLS algorithm performs (28) and (29) recursively from $m = N_m - 2$ to 0 with $\hat{\mathbf{h}}_{\mathrm{s}}(N_m - 1) = \hat{\mathbf{h}}(N_m - 1)$ and $\mathbf{P}_{\mathrm{s}}(N_m - 1) = \mathbf{P}(N_m - 1)$ after the RLS calculation.

TABLE I

COMPUTATIONAL COMPLEXITY

	complex addition	complex multiplication
RLS	$2N_m(N_TD)^2$	$3N_m(N_TD)^2$
S-RLS	$4N_m(N_TD)^2$	$4N_m(N_TD)^2$
SR-RLS	$6N_m(N_TD)^2$	$6N_m(N_TD)^2$

D. Derivation of SR-RLS algorithm

The SR-RLS algorithm can be also derived in the similar way. $\hat{\mathbf{h}}_{\rm r}(m_{\rm a})$ and $\mathbf{P}_{\rm r}(m_{\rm a})$ of the SR-RLS estimation for the i-th OFDM symbol are defined as

$$\hat{\mathbf{h}}_{\rm r}(m_{\rm a}) = \mathbf{R}_{\rm r}^{-1}(m_{\rm a})\mathbf{V}_{\rm r}(m_{\rm a}), \quad \mathbf{P}_{\rm r}(m_{\rm a}) = \mathbf{R}_{\rm r}^{-1}(m_{\rm a}) \tag{30}$$

$$\mathbf{R}_{\rm r}(m_{\rm a}) = \mathbf{R}_{\rm s}(m_{\rm a}) - \sum_{m'=m_{\rm h}}^{m_{\rm t}} \lambda^{|m_{\rm a}-m'|}\mathbf{x}(m')\mathbf{x}^{\rm H}(m'), \tag{31}$$

$$\mathbf{V}_{\rm r}(m_{\rm a}) = \mathbf{V}_{\rm s}(m_{\rm a}) - \sum_{m'=m_{\rm h}}^{m_{\rm t}} \lambda^{|m_{\rm a}-m'|}\mathbf{x}(m')y^*(m'). \tag{32}$$

where $m_{\rm h} = m_{\rm h}(i) = i(N+\Delta_G)$, $m_{\rm t} = m_{\rm t}(i) = (i+1)(N+\Delta_G) - 1$, $m_{\rm a} = m_{\rm a}(i)$ for the estimation at the i-th OFDM symbol, and i is omitted for notation simplicity. For a recursive calculation, let us introduce the following definitions:

$$\hat{\mathbf{h}}_{m_{\rm a},m_{\rm h},m} = \mathbf{R}_{m_{\rm a},m_{\rm h},m}^{-1}\mathbf{V}_{m_{\rm a},m_{\rm h},m}, \tag{33}$$

$$\mathbf{P}_{m_{\rm a},m_{\rm h},m} = \mathbf{R}_{m_{\rm a},m_{\rm h},m}^{-1}, \tag{34}$$

$$\mathbf{R}_{m_{\rm a},m_{\rm h},m} = \mathbf{R}_{m_{\rm a},m_{\rm h},m-1} - \lambda^{|m_{\rm a}-m|}\mathbf{x}_m\mathbf{x}_m^{\rm H}, \tag{35}$$

$$\mathbf{V}_{m_{\rm a},m_{\rm h},m} = \mathbf{V}_{m_{\rm a},m_{\rm h},m-1} - \lambda^{|m_{\rm a}-m|}\mathbf{x}_m y_m^* \tag{36}$$

where $\mathbf{x}_m = \mathbf{x}(m)$, $\mathbf{y}_m = \mathbf{y}(m)$, and $m_{\rm h} \le m \le m_{\rm t}$. Applying the matrix inverse lemma to (34) results in

$$\mathbf{P}_{m_{\rm a},m_{\rm h},m} = \mathbf{P}_{m_{\rm a},m_{\rm h},m-1} - \mathbf{P}_{m_{\rm a},m_{\rm h},m-1}\mathbf{x}_m A_{m_{\rm a},m_{\rm h},m}^{-1}\mathbf{x}_m^{\rm H}\mathbf{P}_{m_{\rm a},m_{\rm h},m-1} \tag{37}$$

$$A_{m_{\rm a},m_{\rm h},m} = -\lambda^{|m_{\rm a}-m|} + \mathbf{x}_m^{\rm H}\mathbf{P}_{m_{\rm a},m_{\rm h},m-1}\mathbf{x}_m. \tag{38}$$

Then, $\hat{\mathbf{h}}_{m_{\rm a},m_{\rm h},m}$ of (33) can be rewritten as

$$\hat{\mathbf{h}}_{m_{\rm a},m_{\rm h},m} = \hat{\mathbf{h}}_{m_{\rm a},m_{\rm h},m-1} + A_{m_{\rm a},m_{\rm h},m}^{-1}\mathbf{P}_{m_{\rm a},m_{\rm h},m-1}\mathbf{x}_m\left(y_m^* - \mathbf{x}_m^{\rm H}\mathbf{h}_{m_{\rm a},m_{\rm h},m-1}\right). \tag{39}$$

The SR-RLS algorithm of (37)-(39) is performed after the S-RLS processing. This is iterated from $m = m_{\rm h}$ to $m_{\rm t}$ with $\hat{\mathbf{h}}_{m_{\rm a};m_{\rm h},m_{\rm h}-1} = \hat{\mathbf{h}}_{\rm s}(m_{\rm a})$ and $\mathbf{P}_{m_{\rm a};m_{\rm h},m_{\rm h}-1} = \mathbf{P}_{\rm s}(m_{\rm a})$. Then, from the definition of (33)-(36), $\hat{\mathbf{h}}_{m_{\rm a};m_{\rm h},m_{\rm t}}$ and $\mathbf{P}_{m_{\rm a};m_{\rm h},m_{\rm t}}$ are equal to $\hat{\mathbf{h}}_{\rm r}(m_{\rm a})$ and $\mathbf{P}_{\rm r}(m_{\rm a})$ of (30), respectively. This process is performed every OFDM symbol.

E. Computational Complexity

Table I compares the computational complexity of the channel estimation algorithms investigated in this paper. The numbers in the table cells are the complexity per one receiver antenna during one packet, which the algorithms with the N_TD taps require. As shown in this table, the complexity of the SR-RLS is about two to three times larger than that of the original RLS algorithm, and they are in the same order.

TABLE II

SIMULATION CONDITION

MIMO antennas ($N_T \times N_R$)	2×2
Modulation	QPSK (Gray mapping), 64 subcarriers OFDM
GI/OFDM symbol duration	16/80
Preamble length	1 OFDM symbol
Channel estimation	16 taps
RLS forgetting factor	0.99
Channel model	9-path Rayleigh (Jakes) 0.8 exponential decay
Inner (EM) iterations	4
Outer iterations	10
Channel coding	half-rate LDPC
Information bits	2048 bits

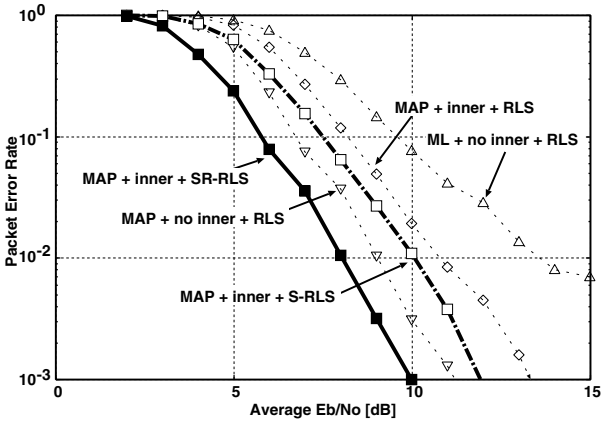

Fig. 4. Effect of the *smoothing* and *removing* ($f_DT_s = 0.02$)

V. COMPUTER SIMULATION

A. Simulation Condition

The simulation conditions are summarized in Table II. The channel model assumed that the maximum delay time is not longer than GI. The normalized Doppler frequency f_DT_s was used as a parameter where f_D and T_s are the Doppler frequency and the OFDM symbol duration, respectively. The forgetting factor of the RLS algorithm was set equally to 0.99 in order to keep the numerical stability of the algorithm and sufficient fading tracking ability. The numbers of inner and outer iterations were set to 4 and 10 respectively, which have been verified in [16].

In the simulation result graphs, "ML" and "MAP" indicate the symbol detection criteria. Only the LDPC decoding is iterated after the ML demodulation in the "ML" case. The receiver with and without the inner loop are denoted by "inner" and "no inner" respectively. Channel estimation methods are denoted by "RLS", "S-RLS" or "SR-RLS".

B. Performance evaluation

Fig. 4 shows the effect of *smoothing* and *removing* on the packet error rate (PER) performance with $f_DT_s = 0.02$. With S-RLS or RLS, the inner loop between the channel estimation and MAP demodulation degrades the PER performance by roughly 1 or 2 dB at PER$= 10^{-2}$, respectively compared to

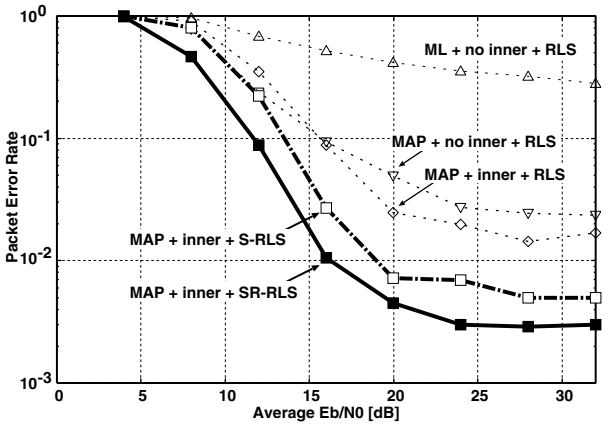

Fig. 5. Effect of the *smoothing* and *removing* ($f_D T_s = 0.03$)

the MAP receiver without the inner loop. On the other hand, the inner loop with SR-RLS improves the PER performance by about 1 dB. This means that the improvement via *smoothing* is not sufficient, and that the channel estimation for the inner loop should use SR-RLS as indicated by the message-passing algorithm. The reason why *removing* is important is as follows. If there is a direct interaction between the channel estimation and the symbol detection at the same OFDM symbol, the iteration of the MAP demodulation and the channel estimation sometimes amplifies the noise through the inaccurate detection and estimation. The SR-RLS channel estimator can avoid this problem by *Removing*.

Fig. 5 shows the PER performance with $f_D T_s = 0.03$. Differently from $f_D T_s = 0.02$, the PER performance degradation through the inner loop occurs only in a low E_b/N_0 region with RLS. On the other hand, the inner loop with either SR-RLS or S-RLS can reduce PER to less than 10^{-2}. Furthermore, SR-RLS achieves E_b/N_0 gains of 4.2dB and 1.9dB at PER=10^{-1} over RLS and S-RLS, respectively. Since the fading tracking is more necessary and the results are plotted in a higher E_b/N_0 region than those with $f_D T_s = 0.02$, the noise amplification problem is less serious with $f_D T_s = 0.03$. Hence, the trend of the results is different from that of $f_D T_s = 0.02$, although *removing* brings about a large improvement.

Note that in both fading conditions, the MAP symbol detection receivers achieve much better performance than the ML symbol detection receiver. There is 3 to 5 dB gain at PER= 10^{-2} with $f_D T_s = 0.02$, and only the MAP receivers can reduce PER to the practical level with $f_D T_s = 0.03$.

VI. Conclusion

This paper has proposed novel channel estimation methods applied to the iterative MAP receiver for the LDPC-coded MIMO-OFDM mobile communications. The receiver performs the joint processing of the signal detection and the channel estimation, which is based on the EM algorithm to perform the MAP detection with practical complexity. By reconsidering the joint processing from the viewpoint of the message-passing algorithm in the factor graph, this paper has proposed *smoothing* and *removing* for the channel estimation. *Smoothing* modifies RLS so that it can use all detected signals for the channel estimation, which is referred to as S-RLS, and *removing* modifies S-RLS so that it removes the direct contribution of detected signals at a targeted OFDM symbol, which is referred to as SR-RLS. The recursive formulas of S-RLS and SR-RLS have been derived theoretically. The computational complexity of SR-RLS is two to three times higher than the original RLS algorithm.

Computer simulations under fast multipath fading conditions have showed that the MAP receiver using the proposed SR-RLS channel estimator outperforms the ones using either the S-RLS or RLS channel estimators. It has been also demonstrated that *removing* is the most effective because it can avoid the noise amplification that can occur in the joint processing of the signal detection and the channel estimation.

References

[1] R. G. Gallager, "Low density parity check codes," *IRE Trans. Inform. Theory*, vol.8, pp.21-28, Jan. 1962.

[2] D. J. C. MacKay and R. M. Neal, "Near shannon limit performance of low density parity check codes," *Electron. Lett.,* vol. 32, No. 18, pp. 1645-1646, Aug. 1996.

[3] G.J.McLachlan and T.Krishnan, *The EM algorithm and extensions,* John Wiley and Sons, 2000.

[4] A. P. Dempster, N. M. Laird, and D. B. Rubin, "Maximum-likelihood from incomplete data via the EM algorithm," *J. R. Stat. Soc.,* Series B, vol. 39, pp. 1-38, 1977.

[5] B. Han, X. Gao, X. You, and M. Weckerle, "Joint Channel Estimation and Symbol Detection for SFBC-OFDM Systems via the EM algorithm," *Commun., 2004 IEEE International Conf.,* vol.6, pp.3148-3152, 20-24 June 2004.

[6] D. K. C. So, and R. S. Cheng, "Improved Iterative EM Receiver for Space Time Coded Systems in Frequency Selective Fading Channel Gain and Order Estimation," *IEEE VTC 2003 Spring*, vol. 2, pp. 847-851, 22-25 April 2003.

[7] S. Y. Park, and C. G. Kang, "Complexity-Reduced Iterative MAP Receiver for Interference Suppression in OFDM-Based Spatial Multiplexing Systems," *IEEE Trans. Veh. Technol.* vol. 53, Issue 5, pp.1316-1326, Sept. 2004.

[8] B. Lu, G. Yue, and X. Wang, "Performance Analysis and Design Optimization of LDPC-Coded MIMO OFDM Systems," *IEEE Trans. Signal Processing*, vol. 52, Issue 2, pp. 348-361, Feb. 2004.

[9] B. Lu, X. Wang, and K. R. Narayanan, "LDPC-Based Space-Time Coded OFDM Systems Over Correlated Fading Channels: Performance Analysis and Receiver Design," *IEEE Trans. Commun.*, vol. 50, Issue 1, pp. 74-88, Jan. 2002.

[10] F. R. Kschischang, B. J. Frey, and H. A. Loeliger, "Factor Graphs and the Sum-Product Algorithm," *IEEE Trans. Inform. Theory*, vol. 47, pp. 498-519, Feb. 2001.

[11] H. A. Loeliger, "An Introduction to Factor Graphs," *IEEE Signal Processing Magazine*, vol. 21, Issue 1, pp. 28-41, Jan. 2004.

[12] J. Proakis, *Digital Communications,* McGraw-Hill, 1995.

[13] G. J. McLachlan, T. Krishnan, *The EM algorithm and Extensions,* WILEY-INTERSIENCE, 1997.

[14] S. Haykin, *Adaptive Filter Theory 3rd edition,* Prentice-Hall, 1996

[15] T. Kashima, K. Fukawa, and H. Suzuki, "Iterative-MAP Adaptive Detection via the EM Algorithm for LDPC-coded MIMO-OFDM Mobile Communications in Fast Fading Channel," in *Proc. IEEE VTC, Stockholm, Sweden*, May-June 2005.

[16] T. Kashima, K. Fukawa, and H. Suzuki, "Adaptive MAP Receiver via the EM algorithm and Message Passings for MIMO-OFDM Mobile Communications," to be published as a paper in *IEEE Jour. on Sel. Area Communi.* Vol.24, No.3, March 2006.